

# Study of Human Serum Albumin Adsorption and Conformational Change on DLC and Silicon Doped DLC Using XPS and FTIR Spectroscopy

Mukhtar H. Ahmed<sup>1\*</sup>, John A. Byrne<sup>1</sup>, James McLaughlin<sup>1</sup>, Waqar Ahmed<sup>2</sup>

<sup>1</sup>Nanotechnology Integrated Bio-Engineering Centre, University of Ulster, Belfast, UK; <sup>2</sup>Institute of Nanotechnology and Bioengineering, University of Central Lancashire, Preston, UK.  
Email: [ahmed-m@email.ulster.ac.uk](mailto:ahmed-m@email.ulster.ac.uk)

Received January 20<sup>th</sup>, 2013; revised March 10<sup>th</sup>, 2013; accepted April 14<sup>th</sup>, 2013

Copyright © 2013 Mukhtar H. Ahmed *et al.* This is an open access article distributed under the Creative Commons Attribution License, which permits unrestricted use, distribution, and reproduction in any medium, provided the original work is properly cited.

## ABSTRACT

Diamond-like carbon (DLC) coatings are extremely useful for creating biocompatible surfaces on medical implants. DLC and silicon doped DLC synthesised on silicon wafer substrate by using plasma enhanced chemical vapour deposition (PECVD). The effects of surface morphology on the interaction of HSA with doped and undoped DLC films have been investigated. The chemical composition of the surface before and after adsorption was analysed using X-ray photoelectron spectroscopy (XPS) and Fourier transform infrared (FTIR). Results showed that silicon incorporation DLC tends to increase of  $sp^3/sp^2$  hybridization ratio by decreasing  $sp^2$  hybridized carbon bonding configurations. Following exposure to solutions containing (0.250  $\mu\text{g/ml}$ ) HSA, the results indicated that significant changes in the C, N and O levels on the surfaces with reducing of the Si2p band at 100 eV. From FTIR spectrum, the peaks occur the following functional groups were assigned as amide I and II groups at 1650  $\text{cm}^{-1}$  and 1580  $\text{cm}^{-1}$ . Both XPS and FTIR spectroscopy confirm that HSA was bound onto the surfaces of the DLC and Si-DLC films via interaction of ionized carboxyl groups and the amino group did not play a significant role in the adsorption of protein. These results from peak intensity show that an adsorbed layer of HSA is higher at high level (19%) silicon doping. Therefore doping of DLC may provide an approach to controlling the protein adsorption.

**Keywords:** Diamond Like Carbon; Si-DLC; HAS; Adsorption; XPS; FTIR

## 1. Introduction

Analysing the interaction of proteins with the surfaces of materials intended for biomedical applications is fundamental for understanding cellular events and the overall host response. Furthermore, the importance of a variety of molecules in the biomedical field is known for several applications, including drug delivery, biomaterials, extracorporeal therapy and solid-phase diagnostics [1]

Both the nature of the biomaterial and the protein has effects on the adsorption process. The most significant surface properties of biomaterials, including the elemental composition, functional groups and surface energy are very important. All of these parameters play a role in enhancing or decreasing the adsorption of proteins or biological compounds during the implant.

Diamond like carbon (DLC) is an ideal candidate for

use as biocompatible coatings on biomedical implants [2] such as coronary artery stents [3], artificial hearts, mechanical heart valves [4], hip and knee replacements [5] and rotary blood pumps [6]. Furthermore DLC possess a unique combination of desirable properties including chemical inertness, high density, hemocompatibility and poor coefficient of friction [7].

Comparative studies improved doped DLC possesses better surface biocompatibility than the undoped counterpart [8]. Thus, to enhance the biocompatibility of DLC, the incorporation of third element dopants like nitrogen [9], fluorine [10], silicon [11] and titanium [12], may be necessary.

Silicon modification has been greatly applied in medical devices and many investigations reported the chemical stability of silicon doped DLC [13]. Silicon incorporation into DLC has been proven to overcome some of the stated drawbacks, including low intrinsic compress-

\*Corresponding author.

sive stress, good adhesion, and mechanical resistance which are beneficial for biomedical applications [14,15]. Investigators have found an improvement in blood compatibility with silicon doped DLC film where a decrease of inflammatory reactions was observed as compared to undoped DLC [16].

To improve the understanding of the fundamentals of protein adsorption, many protein adsorption-modelling approaches have been successfully used.

In this contribution, we explore the coating of silicon wafer substrate with DLC and silicon doped DLC thin films using plasma enhanced chemical vapour deposition (PECVD). The adsorption of human serum albumin (HSA) on these films is investigated, since its adsorption onto surgical instruments and medical devices is likely to dominate *in vivo* due to its abundance in human serum. The physico-chemical properties of adsorption process were evaluated by different techniques using X-ray photoelectron spectroscopy (XPS) and Fourier Transform Infrared (FTIR).

The aim of this study is to illustrate the conformational changes in HSA upon attachment to DLC and Si-DLC surfaces, in order to improve our understanding of the dynamic phenomena in protein adsorption.

## 2. Experimental and Methods

### 2.1. Preparation and Modification of DLC

Before deposition of the films, silicon wafers  $1.5 \times 1.5 \text{ cm}^2$  were cleaned gently and sonicated for 5 min in acetone and isopropanol (1:1) followed by washing with distilled water and then dried using nitrogen gas. Doped and undoped diamond like carbon (DLC) were deposited on cleaned substrates by the radio frequency (RF) 13.56 MHz Plasma Enhanced Chemical Vapour Deposition (PECVD) using a Diavac model 320PA (ACM Ltd.), with negative electrode self-bias voltages set at 400 Volt. The experimental equipment had been described previously in details [17]. The clean substrates are placed in the deposition chamber on top of a water-cooled electrode driven by an RF power supply.

When the chamber pressure reached  $\sim 5 \times 10^{-6}$  Torr an Argon gas flow rate of 60 mL/min was used for substrate surface cleaning. The films were prepared under the following conditions:  $\text{C}_2\text{H}_2$  was used as source gas; Argon (Ar) and tetramethylsilane (TMS) ( $\text{Si}(\text{CH}_3)_4$  [%99.8 Sigma-Aldrich]) were used as dopant source. The argon/acetylene flow ratio (Ar to  $\text{C}_2\text{H}_2$ ) was fixed at (10:20) standard cubic centimetre (sccm), and the deposition time was fixed for (5) minutes. To prepare the Si-DLC samples, the various doping concentrations of silicon were achieved using TMS, and a detail of the parameters is given in **Table 1**.

**Table 1. The deposition conditions of DLC and Si-DLC samples using rf-PECVD system.**

Parameters	Samples			
	DLC	SI	SII	SIII
Pressure in Process $\times 10^{-2}$ (Torr)	0.75	0.89	1.32	1.76
TMS (sccm)	0	2	5	10
Film thickness (nm)	$157 \pm 19$	$173 \pm 13$	$198 \pm 16$	$218 \pm 21$

Bias voltage: 400 volt, deposition time: 5 minute, (TMS): Tetramethylsilane, (sccm): standard centimetre cube per minute, Ar:  $\text{C}_2\text{H}_2$  ratio: 10:20 (sccm), (nm): nanometre, Initial chamber pressure:  $\sim 5 \times 10^{-6}$  Torr, ( $\pm$ ) is SD for  $n = 7$  samples.

### 2.2. Adsorption of Human Serum Albumin (HSA) on DLC and Si-DLC Samples

Human serum albumin (HSA) [from Sigma Aldrich] was prepared in phosphate buffer saline (PBS) [from Sigma-Aldrich] to give solution having concentration of 250  $\mu\text{g/ml}$  and the pH was adjusted at 7.4.

The prepared samples were immersed in the 10 ml of HSA solution (250  $\mu\text{g/ml}$ ) separately in sealed jars and incubated for 60 minute at  $37^\circ\text{C} \pm 1^\circ\text{C}$  using thermostatic shaker bath. After the period time, the samples were then washed twice with distilled water and dried using nitrogen gas.

### 2.3. Surface Characterisation

XPS measurements were obtained using a KRATOS XSAM 800 equipped with an energy analyser. The X-ray source employed was Al  $K\alpha$  X-ray source ( $h\nu 1486 \text{ eV}$ ) generated from aluminium anode operating at the emission voltage at 15 keV and 5 mA. The base pressure within the spectrometer during examination was  $\sim 8 \times 10^{-10}$  bar. All spectra were referenced by setting the hydrocarbon C1s peak to 285.0 eV to compensate for residual charging effects.

The film thickness of the prepared samples was obtained using a stylus profilometer (Dektak 8 Advanced Stylus Profiler Veeco Instruments Inc., USA). Automatic levelling was selected and system based software performed average step height calculations.

The chemical bonding configurations were characterized by Fourier transform infrared spectroscopy FTIR at room temperature using BIORAD Excalibur (FTS 3000 MX series) instrument, to investigate the various chemical vibrational modes the spectrum was recorded in the region of  $4000 - 400 \text{ cm}^{-1}$  and 60 scans were accumulated at a resolution of  $4 \text{ cm}^{-1}$ . In all of the FTIR experiments the background spectrum was collected before the actual sample analysis using the relevant unattached coated samples with Human serum albumin (HSA) and

this signature was subsequently removed from the sample scan. The subsequent analysis of the attached HSA on the DLC and Si-DLC samples was performed.

### 3. Results and Discussion

#### 3.1. Surface Characterisation of Prepared Samples

The film thicknesses of DLC and Si-DLC samples have been obtained and the values were arranged from  $\sim(157 - 218)$  nm, the growth rate of film deposition was around  $(38 \pm 6)$  nm·min<sup>-1</sup> (**Table 1**).

**Figure 1** shows the survey scan of XPS spectra of doped and undoped DLC. The main peaks were observed at  $\sim 285.1$  eV, and  $\sim 531.4$  eV, corresponding to C1s and O1s, bands, respectively. The addition peak was revealed at 100.7 eV [in case of silicon doped DLC] which attributed to Si2p.

C1s spectrum of DLC has been deconvoluted in to three different peaks. The first band located at 284.7 eV, is related to the sp<sup>2</sup> hybridized carbon (C=C). A band at 285.3 eV, is corresponded to a sp<sup>3</sup> carbon (C-C), and last peak was obtained at 287.4 eV, can be related to the (CO) bonds (**Figure 2**). The carbon atom percentage in the DLC is determined as 86.70% (**Table 2**).

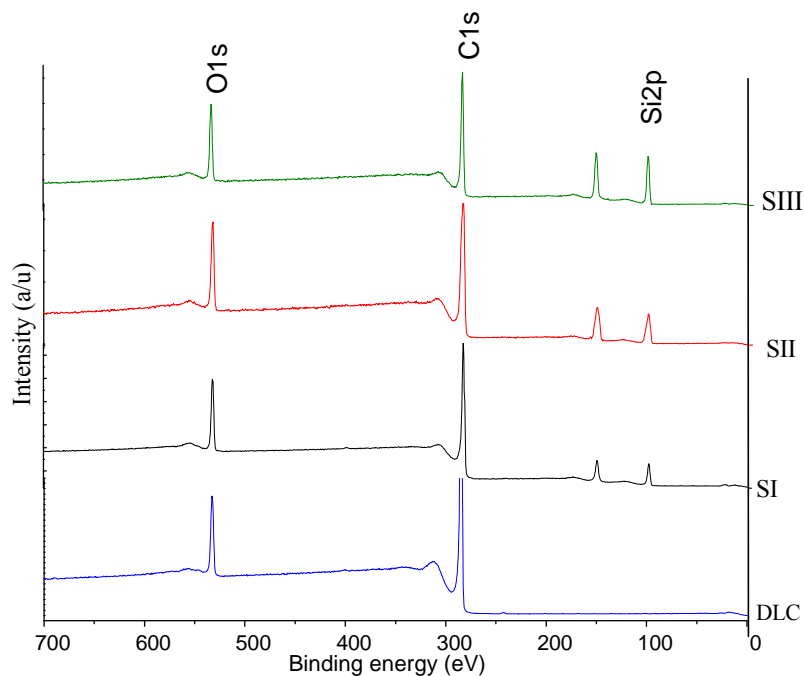
It has been observed that the presence of silicon in the film affected the binding energy by causing a slight lowering in the energy accompanied by a broadening of the C1s peaks with FWHM of 2.5 eV, which increased with increasing silicon concentration in the films. The C1s

spectrum of Si-DLC yielded four deconvoluted peaks; at 283.9 eV [Si-C], 284.7 eV [C=C], 285.3 eV [C-C], 287.3 eV [CO] [18]. On the other hand, the intensity of both Si-C and C-C increased with increasing the silicon concentration in the films, the results agree with those obtained by Zhao *et al.* [19].

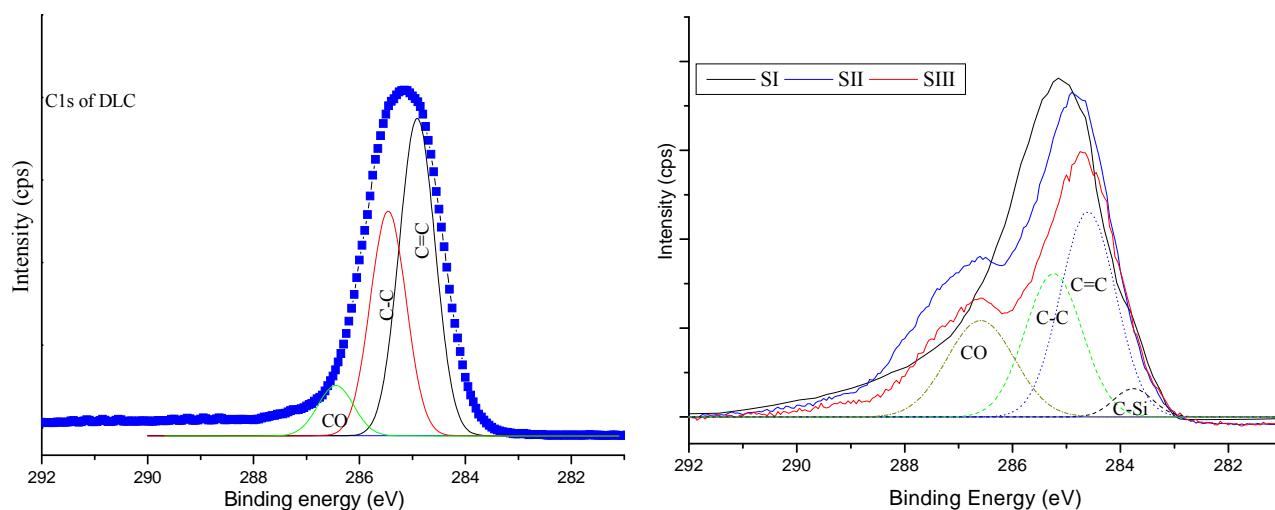
The properties of the DLC thin films depend mainly on its structure resulting from combination of sp<sup>3</sup> bonding (Diamond form) and sp<sup>2</sup> (graphite form). The sp<sup>3</sup> to sp<sup>2</sup> ratio is dependent on the deposition process and its parameters. The incorporation of silicon into DLC leads to the decrease of C=C (Sp<sup>2</sup>) bonded with increase of C-Si contribution, while the amount of the C-C bonding (sp<sup>3</sup>) remained relatively unaltered. The results show that silicon atoms preferentially substitute the sp<sup>2</sup> hybridized carbon atoms during film formation. Then one may conclude that silicon content can increase the sp<sup>3</sup>/sp<sup>2</sup> ratio in the film (**Figure 3**). This tends to improve the compatibility of the implant with blood components [20].

The XPS O1s spectra of DLC and Si-DLC samples were located at  $\sim 531$  eV (**Figure 4**). Deconvolution of the O1s band gave two sub peaks around 531 eV and 532 eV, which are attributed to (C=O) and (C-O) bond in the film structure, respectively.

The results of the XPS analysis of the O1s region of the Si-DLC samples showed that the oxygen concentration in the films increases with increasing silicon flow rate, (**Table 2**). The obtained results are in good agreement with those provided previously determined values [11].



**Figure 1.** XPS survey scans for DLC and Si-DLC (SI, SII and SIII) samples.


**Figure 2.** XPS C1s spectra deconvolution of DLC and Si-DLC samples.

**Table 2.** XPS survey data (atomic percentage) for the elements on to surface of samples before and after adsorption of HAS.

Samples	Peak designation	Before adsorption of HSA			After adsorption of HSA		
		Band (eV)	At. % Conc.	FWHM (eV)	Band (eV)	At. % Conc.	FWHM (eV)
DLC	C1s	285.1	86.7	1.5	284.9	62.5	2.0
	O1s	531.4	13.3	2.4	532.1	32.6	2.2
	N1s				399.7	4.9	1.9
SI	C1s	284.9	81.9	1.8	285.0	62.7	2.1
	O 1s	532.1	13.7	2.3	532.0	31.9	2.1
	Si2p	100.7	4.4	1.6			
SII	N1s				399.5	5.4	2.2
	C1s	284.9	76.3	2.1	284.9	62.1	2.3
	O1s	532.4	14.1	2.2	531.9	32.7	2.0
SIII	Si2p	100.3	9.6	2.2			
	N1s				399.8	5.2	2.1
	C1s	284.7	68.5	2.5	284.7	62.0	2.3
	O1s	531.7	14.7	2.1	532.0	32.5	2.1
	Si2p	100.4	16.8	3.0			
	N1s				399.8	5.5	2.2

On the other hand, the band related to silicon atom (Si2p) appeared at around 101 eV. The fitted band of Si2p gives two sub-peaks centred at 100.6 eV and 102.3 eV can be assigned to Si-C and Si-O bonds, respectively. The quantitative analysis of atomic percentage of silicon content DLC gives 4.4, 9.6 and 16.8 for SI, SII and SIII, respectively (**Table 2**).

**Figure 5** shows the FTIR spectrum of doped and undoped DLC samples. Bands located at around  $1450\text{ cm}^{-1}$

and  $896\text{ cm}^{-1}$  are assigned to the stretching and bending of C-C  $\text{sp}^3$  hybridization respectively, and a medium band at  $1210\text{ cm}^{-1}$  can also be assigned to the  $\text{sp}^3$  bond of carbon hybridisation [21]. This indicates the formation of tetrahedral carbon structures in the DLC films and the inclusion of hydrogen. The peak at  $\sim 727\text{ cm}^{-1}$  belongs to the out of plane bending configuration of the graphite like carbon [22]. A weak peak at  $1624\text{ cm}^{-1}$  is assigned to carbon double bond hybridization. In addition to the

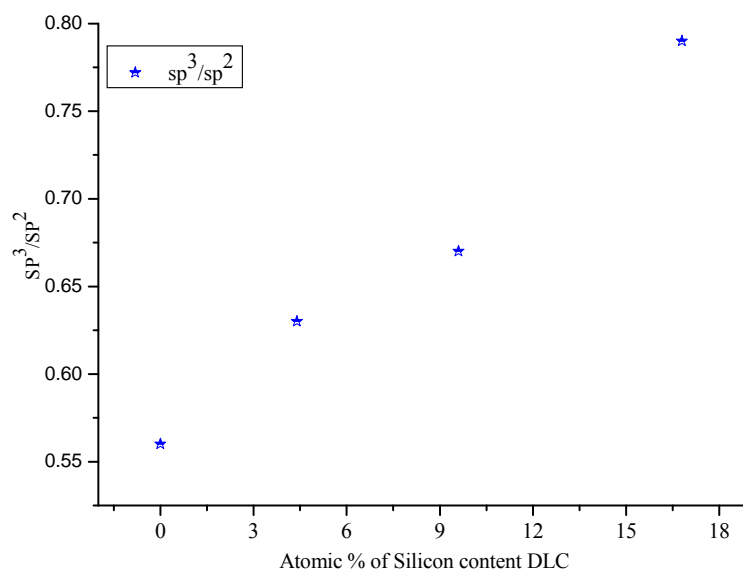


Figure 3. sp<sup>3</sup>/sp<sup>2</sup> ratio in relation to atomic present of silicon content DLC.

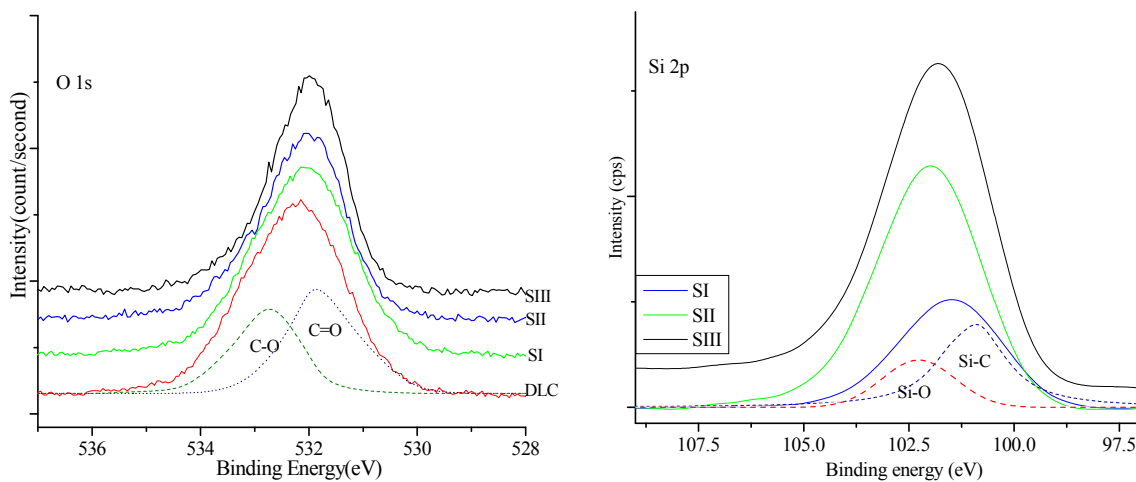


Figure 4. The XPS O1s and Si2p spectra of deposited samples.

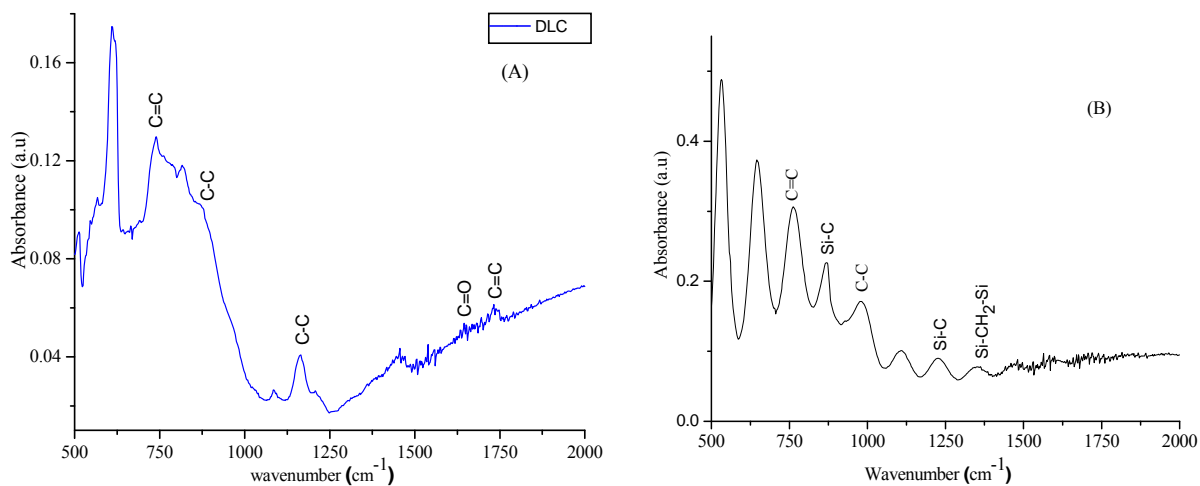


Figure 5. FTIR spectra of DLC (A) and Si-DLC (B).

bands at  $905\text{ cm}^{-1}$  and  $1192\text{ cm}^{-1}$  which is return to the C-C bonds, too. For Si-DLC samples, the bands have been detected at  $880\text{ cm}^{-1}$ , attributed to the Si-CH bond [23]. in addition, the deformation vibration of Si-CH<sub>3</sub> bond was observed at  $1263\text{ cm}^{-1}$  and a band appeared at around  $1359\text{ cm}^{-1}$  suggested the presence of stretching vibration of Si-CH<sub>2</sub>-Si bonds. The results are agree with those achieved by Finer *et al.* [24].

### 3.2. Characterization of Surfaces after HSA Adsorption

XPS was used to investigate the chemical surface composition during the HSA adsorption. The survey scan XPS spectrum of adsorbed HSA on the DLC and Si-DLC surfaces is presented in **Figure 6**. The results showed that a new signal at 400 eV has observed is assigned to N1s band, and the C1s band intensity was significantly changed, along with a reduction in the Si2p intensity (in case of Si-DLC). Furthermore, a weak band was detected at 164.1 eV in the high-resolution analysis of the S2p which can be attributed to sulphur atoms in cysteine amino acid [25]. These data indicate the presence of the protein on the surfaces [26].

High resolution analysis of the C1s peak after adsorption of protein was quite different from the samples prior to protein adsorption. The deconvolution of the C1s peak gave four different bands. The first component located at  $\sim 285.2\text{ eV}$  which assigned to saturated and unsaturated hydrocarbon groups. A peak at  $286.7\text{ eV}$  is related to C-NH amine groups and the last peak detected at around  $288.4\text{ eV}$  is for the peptide bond HN-C=O, (**Figure 7**).

After peak fitting of the N1s core-level spectrum, three

deconvoluted peaks were observed at  $399.7\text{ eV}$  (73%), is attributed to (C-N), a peak showed at  $401.7\text{ eV}$  (19%) assigned to N-C=O and N-H bonded [27], and the third band was appeared at  $402.8\text{ eV}$  (8%) is returned to positively charged amines (NH<sub>3</sub><sup>+</sup>). The NH<sub>3</sub><sup>+</sup> component of N1s spectrum of Si-DLC samples shifts to a higher binding energy with a slight increase in band area, compared to the same band in undoped DLC. This might evidence that the HSA was adsorbed on to surfaces via carboxylic acid group [17].

The O1s band after protein adsorption is similar to that without protein, suggesting that the most of the signal is attributable to carbon oxides and surface OH groups (**Figure 7**). The amount of protein adsorbed onto a surface, can be related to the intensity of C1s peak. Hence, based on the C1s intensity, the relative amount of adsorbed HSA increases with increasing silicon doped DLC. Therefore, doping of DLC may allow control of protein adsorption to the surface.

### Fourier Transform Infrared (FTIR)

FTIR spectroscopy can be used for identification of the functional group and showing different vibrational modes of various bonds which are present in the film. **Figure 8** shows the FTIR spectrum of free and bounded HSA on to surface of coated DLC. The bands centred at around  $1650\text{ cm}^{-1}$  and  $1550\text{ cm}^{-1}$ , which correspond to amide I and amide II, respectively. The location of both the Amide bond orientation are sensitive to the secondary structure of a protein, because both groups of C=O and the N-H bonds are involved in the hydrogen bonding that takes place between the different elements of secondary

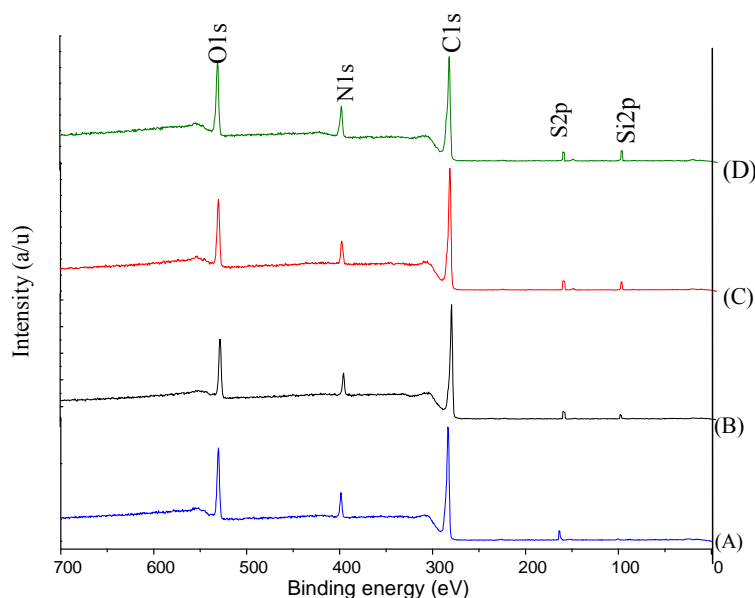


**Figure 6.** The XPS survey scan for DLC and Si-DLC surfaces.

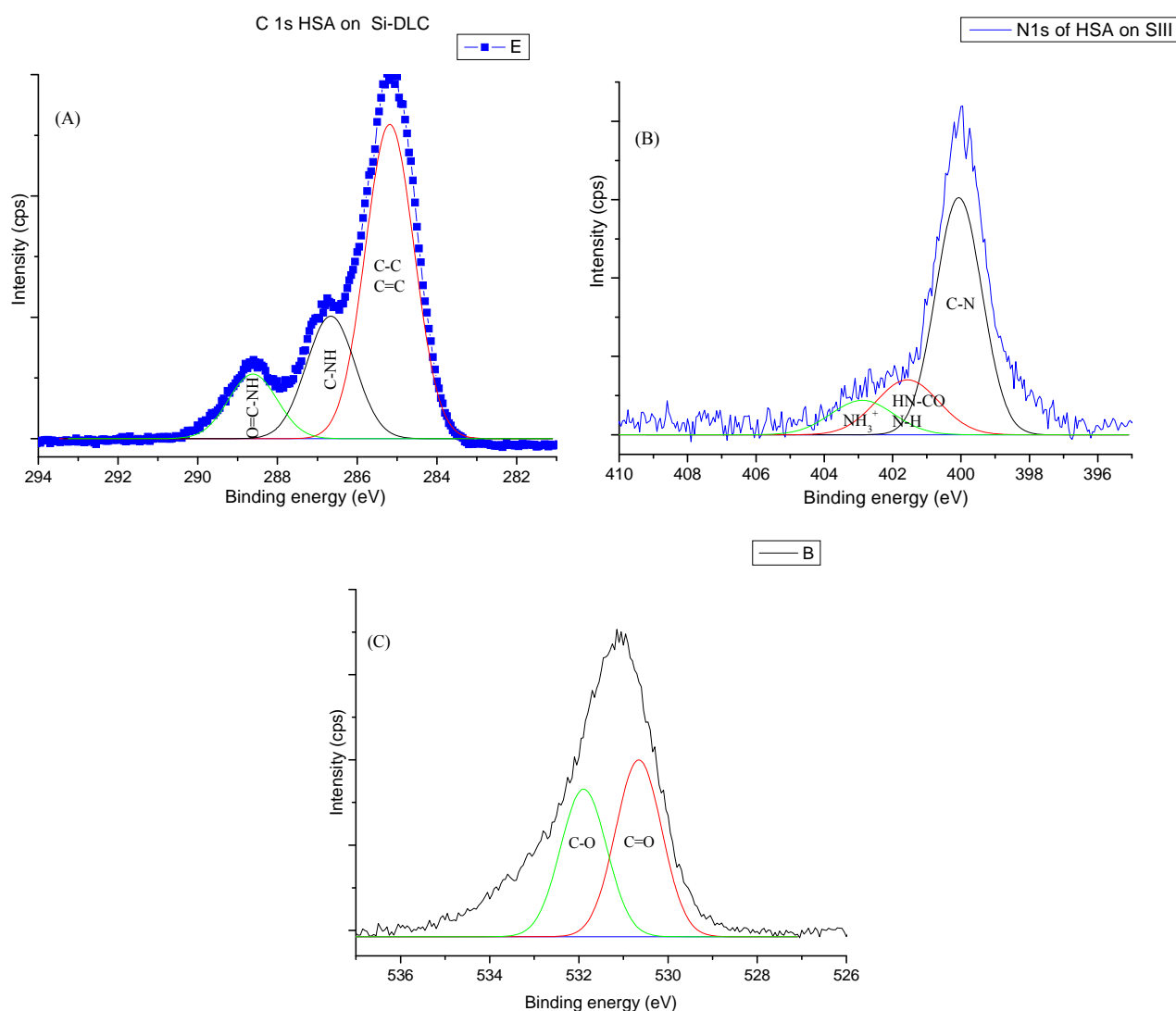


Figure 7. The XPS C1s (A), N1s (B) and O1s (C) spectra for adsorbed HSA onto DLC and Si-DLC.

structure [28]. The Amide I band of free HSA, is located at  $1650\text{ cm}^{-1}$ , whilst in case of adsorbed HSA onto doped DLC, the same band observed at around  $1641\text{ cm}^{-1}$ . A quantitative analysis of the amide I region can be estimated by curve fitting confirms the gradual evolution in the secondary structure content.

To investigate changes in the secondary structure of HSA after it is conjugated to the coated DLC surface, the deconvolution and second derivative of amide I band has been applied. Spectral deconvolution resolved four peaks for the amide I band for the free HSA, (Figure 9). A band located at  $1612\text{ cm}^{-1}$  which is correlated to aromatic rings. The second component was seen at  $1629\text{ cm}^{-1}$  and can be attributed to  $\beta$ -sheet structure [29]. Band at around  $1663\text{ cm}^{-1}$  is related to  $\alpha$ -helix [30], and the last fitted peak detected at  $1675\text{ cm}^{-1}$  which is return to anti-parallel  $\beta$ -sheets components [31]. The quantitative ana-

lysis of the amide I spectra of free HSA peptide indicates that there is more than 57% of  $\alpha$ -helix and ~17% of  $\beta$ -sheet conformation (Table 3). The obtained results are in good agreement with the data reported by Bouhekkka *et al.* [32].

Whilst the deconvoluted of the same band after adsorption of HSA on to surface of samples, gives five secondary peaks at  $\sim 1611\text{ cm}^{-1}$  (aromatic ring),  $\sim 1630\text{ cm}^{-1}$  ( $\beta$ -sheet),  $1644\text{ cm}^{-1}$  (random coil),  $1664\text{ cm}^{-1}$  ( $\alpha$ -helix) and  $\sim 1679\text{ cm}^{-1}$  ( $\beta$ -sheet anti parallel). The  $\beta$ -sheet is slightly increased from (17% to ~25%). Furthermore, a decrease in  $\alpha$ -helical contribution is observed from (57% to 45%) (Figure 9). These could be attributable to the enhancing of HSA aggregation on to surfaces. The results are similar to those obtained by Khan *et al.* [33].

The amide II is arising from the in-plane N-H bending mode (40 - 60)% of the potential energy, and the rest of

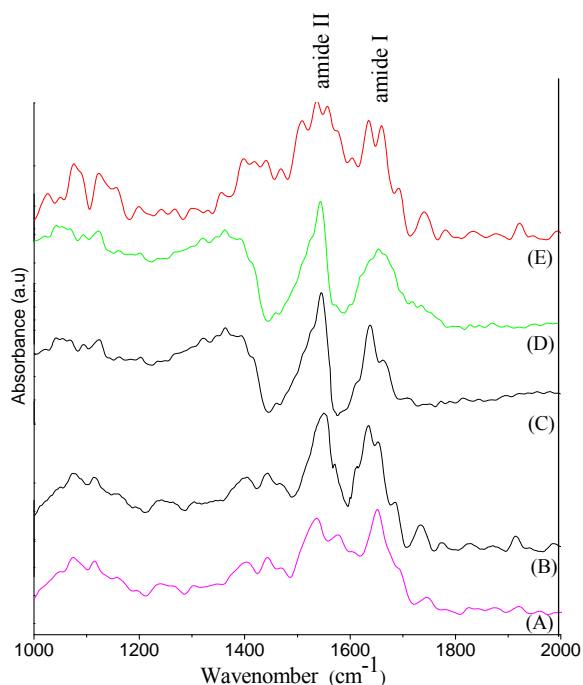


**Figure 8.** FTIR Spectra of HSA before (A) and after adsorbed on DLC (B), SI (C), SII (D) and SIII (E) surfaces.

the potential energy emerges from the C-N (20 - 40%) and C-C about 10% stretching vibrations [34]. In case of free HSA, the amide II shows a maximum of absorbance that shifts from 1559  $\text{cm}^{-1}$  to lower wavenumbers (1553  $\text{cm}^{-1}$ ) upon HSA adsorption onto DLC-coated surfaces. This shift can be correlated to the change of protein conformation during the adsorption [35]. In all these processes a hydrogen bond plays a dominant role in deciding the structure of the aggregate [36].

#### 4. Conclusions

The results indicated that DLC films are established to consist of a mixture of tetrahedral ( $\text{sp}^3$ ) and trigonal ( $\text{sp}^2$ ) bonding. XPS data showed that the  $\text{sp}^3/\text{sp}^2$  ratio increases with increasing silicon concentration in the DLC film. Furthermore, FTIR analysis showed that silicon incorporation DLC gives rise to the formation of Si-C bond, which tends to increase in the fraction of  $\text{sp}^3$  bonded carbon in DLC film.

Followed by exposure to protein, a new band of nitrogen (N1s) appeared at the XPS spectra of the doped and undoped DLC surfaces. As well as a specific broad peak was observed at  $\sim 288.4$  eV could be assigned to peptide

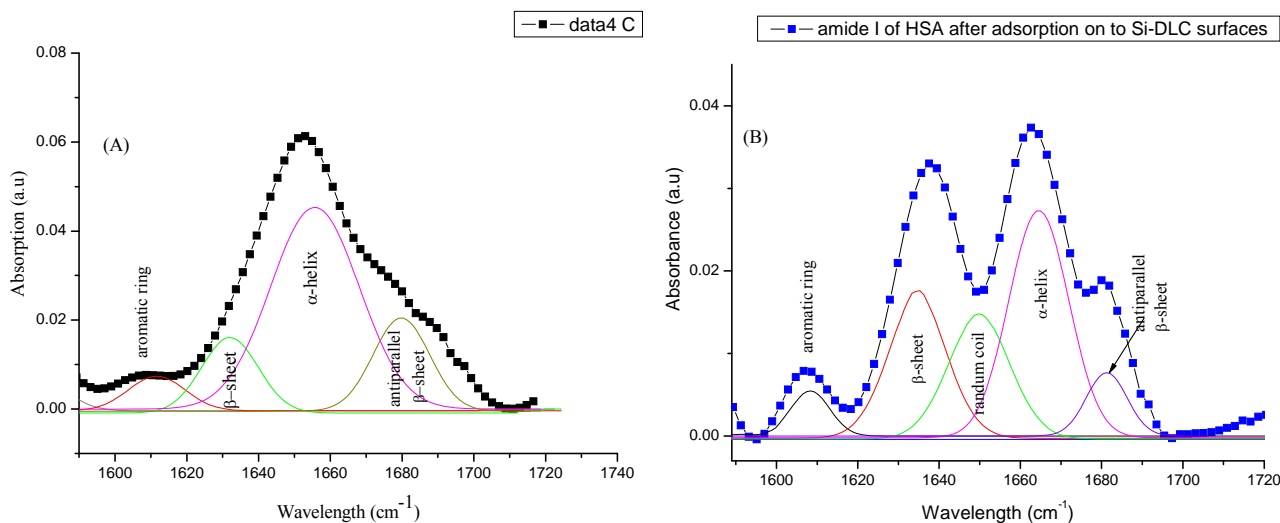


**Figure 9.** Curve-fitting analysis of the amide I in FTIR; for free HSA (A) and adsorbed on SIII (B).

**Table 3.** FTIR analysis of the amide I band of free and adsorbed HSA onto DLC and Si-DLC samples.

Amide I bands	Free HSA		HSA adsorbed on DLC		HSA adsorbed on SIII	
	( $\text{cm}^{-1}$ )	Band %	( $\text{cm}^{-1}$ )	Band %	( $\text{cm}^{-1}$ )	Band %
Aromatic	1612	13.74	1611	12.42	1609	11.83
$\beta$ -sheet	1629	17.86	1631	25.82	1633	26.91
Random coil			1644	7.1	1645	8.3
$\alpha$ -helix	1663	57.86	1664	45.52	1662	44.3
$\beta$ -sheet anti parallel	1675	10.54	1679	9.14	1681	8.66



bond. In addition of, the presence of protonated amino groups ( $\text{NH}_3^+$ ) at 402.6 eV, this might suggesting that HSA bounded on the surfaces through the carboxyl group and the amino group has not interact strongly with the surface.

FTIR spectra revealed the presence of amide I and II at  $1650\text{ cm}^{-1}$  and  $1559\text{ cm}^{-1}$  belonging to protein. The results also suggested that relatively the adsorbed amount of HSA increased with increasing of silicon content on the DLC film. The presence studies have revealed that modifying the surface of DLC by incorporation of silicon can improve its biocompatibility of the implant; however, further studies are required to obtain a better understanding of protein adsorption *in vivo*.

## 5. Acknowledgements

The authors would like to thank all of the staff at Northern Ireland Bio-Engineering Centre (NIBEC), University of Ulster for their support, and also thanks to Sandra Adamson at LG, for her technical assistance.

## REFERENCES

- [1] C. M. Alves, R. L. Reis and J. A. Hunt, "The Competitive Adsorption of Human Proteins onto Natural-Based Biomaterials," *Journal of the Royal Society Interface*, Vol. 7, No. 50, 2010, pp. 1367-1377. [doi:10.1098/rsif.2010.0022](https://doi.org/10.1098/rsif.2010.0022)
- [2] T. Hasebe, A. Hotta, H. Kodama, A. Kamijo, K. Takahashi and T. Suzuki, "Recent Advances in Diamond-Like Carbon Films in the Medical and Food Packing Fields," *New Diamond and Fornier Carbon Technology*, Vol. 17, No. 6, 2007, pp. 263-279.
- [3] H. W. Choi, R. H. Dauskardt, S. C. Lee, K. R. Lee and K. H. Oh, "Characteristic of Silver Doped DLC Films on Surface Properties and Protein Adsorption," *Diamond & Related Materials*, Vol. 17, No. 3, 2008, pp. 252-257. [doi:10.1016/j.diamond.2007.12.034](https://doi.org/10.1016/j.diamond.2007.12.034)
- [4] D. Grimanelis, S. Yang, O. Bohme, E. Roman, A. Alberdi, D. G. Teer and J. M. Albella, "Carbon Based Coating for High Temperature Cutting Tools," *Applications, Diamond and Related Materials*, Vol. 11, No. 2, 2002, pp. 176-184. [doi:10.1016/S0925-9635\(01\)00566-0](https://doi.org/10.1016/S0925-9635(01)00566-0)
- [5] J. I. Onate, M. Comin, I. Braceras, A. Garcia, J. L. Viviente, M. Brizuela, N. Garagorri, J. L. Perisb and J. I. Alava, "Wear Reduction Effect on Ultra-High-Molecular-Weight Polyethylene by Application of Hard Coatings and Ion Implantation on Cobalt Chromium Alloy, as Measured in a Knee Wear Simulation Machine," *Surface Coatings Technology*, Vol. 142-144, 2001, pp. 1056-1062. [doi:10.1016/S0257-8972\(01\)01074-X](https://doi.org/10.1016/S0257-8972(01)01074-X)
- [6] A. Alanazi, C. Nojiri, T. Kido, T. Noguchi, Y. Ohgoe, T. Matsuda, K. Hirakuri, A. Funakubo, K. Sakai and Y. Fukui, "Engineering Analysis of Diamond-Like Carbon Coated Polymeric Materials for Biomedical Applications," *Artificial Organs*, Vol. 24, No. 8, 2000, pp. 624-627. [doi:10.1046/j.1525-1594.2000.06576.x](https://doi.org/10.1046/j.1525-1594.2000.06576.x)
- [7] R. K. Roy, H. W. Choi, J. W. Yi, M. W. Moon, K. R. Lee, D. K. Han, J. H. Shin, A. Kamijo and T. Hasebe, "Hemocompatibility of Surface-Modified, Silicon-Incorporated, Diamond-Like Carbon Films," *Acta Biomaterialia*, Vol. 5, No. 1, 2009, Article ID: 249256. [doi:10.1016/j.actbio.2008.07.031](https://doi.org/10.1016/j.actbio.2008.07.031)
- [8] S. C. H. Kwok, W. Zhang, G. J. Wan, D. R. McKenzie, M. M. M. Bilek and P. K. Chu, "Hemocompatibility and Anti-Bacterial Properties of Silver Doped Diamond-Like Carbon Prepared by Pulsed Filtered Cathodic Vacuum Arc Deposition," *Diamond & Related Materials*, Vol. 16, No. 4-7, 2007, pp. 1353-1360. [doi:10.1016/j.diamond.2006.11.001](https://doi.org/10.1016/j.diamond.2006.11.001)
- [9] M. H. Ahmed and J. A. Byrne, "Effect of Surface Structure and Wettability of DLC and N-DLC Thin Films on Adsorption of Glycine," *Applied Surface Science*, Vol. 258, No. 12, 2012, pp. 5166-5174. [doi:10.1016/j.apsusc.2012.01.162](https://doi.org/10.1016/j.apsusc.2012.01.162)
- [10] M. H. Ahmed, J. A. Byrne and J. McLaughlin, "Evaluation of Glycine Adsorption on Diamond Like Carbon (DLC) and Fluorinated DLC Deposited by Plasma-Enhanced Chemical Vapour Deposition (PECVD)," *Surface & Coatings Technology*, Vol. 209, 2012, pp. 8-14. [doi:10.1016/j.surfcoat.2012.07.011](https://doi.org/10.1016/j.surfcoat.2012.07.011)
- [11] M. Ahmed, A. J. Byrne, J. McLaughlin, A. Elhissi, D. A. Phoenix and W. Ahmed, "Vibrational and AFM Studies of Adsorption of Glycine on DLC and Silicon-Doped DLC," *Journal of Materials Science*, Vol. 47, No. 4, 2012, pp. 1729-1736. [doi:10.1007/s10853-011-5952-3](https://doi.org/10.1007/s10853-011-5952-3)
- [12] C. Liu, G. Q. Li, W. X. Chen, Z. X. Mu, C. W. Zhang and L. Wang, "The Study of Doped DLC Films by Ti Ion Implantation," *Thin Solid Films*, Vol. 475, No. 1-2, 2005, pp. 279-282. [doi:10.1016/j.tsf.2004.08.051](https://doi.org/10.1016/j.tsf.2004.08.051)
- [13] G. H. Hsiue, S. D. Lee, P. C. T. Chang and C. Y. Kao, "Surface Characterization and Biological Properties Study of Silicone Rubber Membrane Grafted with Phospholipid as Biomaterial via Plasma Induced Graft Copolymerization," *Journal of Biomedical Materials Research*, Vol. 42, No. 1, 1998, pp. 134-147. [doi:10.1002/\(SICI\)1097-4636\(199810\)42:1<134::AID-JB M17>3.0.CO;2-L](https://doi.org/10.1002/(SICI)1097-4636(199810)42:1<134::AID-JB M17>3.0.CO;2-L)
- [14] J. C. Damasceno, S. S. Camargo Jr., F. L. Freire Jr. and R. Carius, "Deposition of Si-DLC Films with High Hardness, Low Stress and High Deposition Rates," *Surface and Coatings Technology*, Vol. 133-134, 2000, pp. 247-252. [doi:10.1016/S0257-8972\(00\)00932-4](https://doi.org/10.1016/S0257-8972(00)00932-4)
- [15] N. Moolsradoo, S. Abe and S. Watanabe, "Thermal Stability and Tribological Performance of DLC-SiO<sub>2</sub> Films," *Advances in Materials Science and Engineering*, Vol. 2011, 2011, Article ID: 483437.
- [16] S. Kelly, E. M. Regan, J. B. Uney, A. D. Dick, J. P. McGeehan, E. J. Mayer and F. Claeysens, "Patterned Growth of Neuronal Cells on Modified Diamond-Like Carbon Substrates," *Biomaterials*, Vol. 29, No. 24-25, 2008, pp. 2573-2580. [doi:10.1016/j.biomaterials.2008.03.001](https://doi.org/10.1016/j.biomaterials.2008.03.001)
- [17] M. Ahmed, J. Anthony Byrne and J. A. D. McLaughlin, "Glycine Adsorption onto DLC and N-DLC Thin Films

- Studied by XPS and AFM,” *e-Journal of Surface Science and Nanotechnology*, Vol. 7, 2009, pp. 217-224. [doi:10.1380/ejsnt.2009.217](https://doi.org/10.1380/ejsnt.2009.217)
- [18] A. Bendavid, P. J. Martin, C. Comte, E. W. Preston, A. J. Haq, F. S. M. Ismail and R. K. Singh, “The Mechanical And Biocompatibility Properties of DLC-Si Films Prepared by Pulsed DC Plasma Activated Chemical Vapor Deposition,” *Diamond & Related Materials*, Vol. 16, No. 8, 2007, pp. 1616-1622. [doi:10.1016/j.diamond.2007.02.006](https://doi.org/10.1016/j.diamond.2007.02.006)
- [19] Q. Zhao, Y. Liu, C. Wang and S. Wang, “Bacterial Adhesion on Silicon-Doped Diamond-Like Carbon Films,” *Diamond and Related Materials*, Vol. 16, No. 8, 2007, pp. 1682-1687. [doi:10.1016/j.diamond.2007.03.002](https://doi.org/10.1016/j.diamond.2007.03.002)
- [20] R. K. Roy, S. J. Park, H. W. Choi, K. R. Lee, J. H. Kim, D. K. Han, J. H. Shin, H. G. Kim, S. H. Ahn, J. G. Kim, S. J. Park and K. R. Lee, “Hemocompatibility of Surface Modified Si Incorporated Diamond-Like Carbon Films,” *Thin Solid Films*, Vol. 482, 2005, pp. 299-304.
- [21] R. Paul, S. N. Das, S. Dalui, R. N. Gayen, R. K. Roy, R. Bhar and A. K. Pal, “Synthesis of DLC Films with Different  $sp^2/sp^3$  Ratios and Their Hydrophobic Behaviour,” *Journal of Physics D: Applied Physics*, Vol. 41, No. 5, 2008, Article ID: 055309. [doi:10.1088/0022-3727/41/5/055309](https://doi.org/10.1088/0022-3727/41/5/055309)
- [22] W. J. Hsieh, P. S. Shih, C. C. Lin, C. Y. Wang and H. C. Shi, “Structure and Optical Property of the a-C:N Films Synthesized by Filtered Cathode Vacuum Arc,” *Surface and Coatings Technology*, Vol. 200, No. 10, 2006, pp. 3175-3178. [doi:10.1016/j.surfcoat.2005.07.038](https://doi.org/10.1016/j.surfcoat.2005.07.038)
- [23] M. N. Huda, Y. Yan and M. M. Al-Jassim, “On the Existence of Si-C Double Bonded Graphene-Like Layers,” *Chemical Physics Letters*, Vol. 479, No. 4-6, 2009, pp. 255-258. [doi:10.1016/j.cplett.2009.08.028](https://doi.org/10.1016/j.cplett.2009.08.028)
- [24] N. Fainer, Y. Romyantsev, M. Kosinova, E. Maximovski, V. Kesler, V. Kirienko and F. Kuznetsov, “Low-k Dielectrics on Base of Silicon Carbon Nitride Films,” *Surface and Coatings Technology*, Vol. 201, No. 22, 2007, pp. 9269-9274. [doi:10.1016/j.surfcoat.2007.04.046](https://doi.org/10.1016/j.surfcoat.2007.04.046)
- [25] H. Yoneyama and T. Torimoto, “Titanium Dioxide/Adsorbent Hybrid Photocatalysts for Photodestruction of Organic Substances of Dilute Concentrations,” *Catalysis Today*, Vol. 58, No. 2-3, 2000, pp. 133-140.
- [26] T. Kesvatera, B. Jonsson, A. Telling, V. Tougu, H. V. E. Thulin and S. Linse, “A Protein Optimized for Calcium Binding at Neutral pH,” *Biochemistry*, Vol. 40, No. 50, 2001, pp. 15334-15340.
- [27] H. J. Kim, I.-S. Bae, S.-J. Cho, J.-H. Boo, B.-C. Lee, J. Heo, I. Chung and B. Hong, “Synthesis and Characteristics of  $NH_2$ -Functionalized Polymer Films to Align and Immobilize DNA Molecules N-Containing Moieties Could Be Useful,” *Nanoscale Research Letters*, Vol. 7, 2012, pp. 30-37. [doi:10.1186/1556-276X-7-30](https://doi.org/10.1186/1556-276X-7-30)
- [28] M. Bouchard, J. Zurdo, E. J. Nettleton, C. M. Dobson, and C. V. Robinson, “Formation of Insulin Amyloid Fibrils Followed by FTIR Simultaneously with CD and Electron Microscopy,” *Protein Science*, Vol. 9, No. 10, 2000, pp. 1960-1967. [doi:10.1110/ps.9.10.1960](https://doi.org/10.1110/ps.9.10.1960)
- [29] M. Jackson and H. H. Mantsch, “The Use and Misuse of FTIR Spectroscopy in the Determination of Protein Structure,” *Critical Reviews in Biochemistry and Molecular Biology*, Vol. 30, No. 2, 1995, pp. 95-120. [doi:10.3109/10409239509085140](https://doi.org/10.3109/10409239509085140)
- [30] K. L. Munro, K. R. Bamberg, E. A. Carter, L. Puskar, M. J. Tobin, B. R. Wood and C. T. Dillon, “Synchrotron Radiation Infrared Microspectroscopy of Arsenic-Induced Changes to Intracellular Biomolecules in Live Leukaemia Cells,” *Vibrational Spectroscopy*, Vol. 53, No. 1, 2010, pp. 39-44. [doi:10.1016/j.vibspec.2010.02.004](https://doi.org/10.1016/j.vibspec.2010.02.004)
- [31] C. Chadeaux, A.-S. L. Ho, L. Bellot-Gurlet and I. Reiche, “Curve-Fitting Micro-ATR-FTIR Studies of the Amide I and II Bands of Type I Collagen Archaeological Bone Materials,” *e-Preservation Science*, Vol. 6, 2009, pp. 129-137.
- [32] A. Bouhekkka and T. Burgi, “In Situ ATR-IR Spectroscopy Study of Adsorbed Protein: Visible Light Denaturation of Bovine Serum Albumin on  $TiO_2$ ,” *Applied Surface Science*, Vol. 261, 2012, pp. 369-374. [doi:10.1016/j.apsusc.2012.08.017](https://doi.org/10.1016/j.apsusc.2012.08.017)
- [33] M. W. Khan, Z. Rasheed, W. A. Khan and R. Ali, “Biochemical, Biophysical, and Thermodynamic Analysis of in Vitro Glycated Human Serum Albumin,” *Biochemistry (Moscow)*, Vol. 72, No. 2, 2007, pp. 146-152. [doi:10.1134/S0006297907020034](https://doi.org/10.1134/S0006297907020034)
- [34] M. L. Gulrajani, K. P. Brahma, P. S. Kumar and R. Purwar, “Application of Silk Sericin to Polyester Fabric,” *Journal of Applied Polymer Science*, Vol. 109, No. 1, 2008, pp. 314-321. [doi:10.1002/app.28061](https://doi.org/10.1002/app.28061)
- [35] M. Dumitrascu, V. Meltzer, E. Sima, M. Virgolici, M. G. Albu, A. Fikai, V. Moise, R. Minea, C. Vancea, A. Scarioreanu and F. Scarlat, “Characterization of Electron Beam Irradiated Collagen-Polypropylidone (PVP) and Collagen-Dextran (DEX) Blends,” *Digest Journal of Nanomaterials and Biostructures*, Vol. 6, 2011, pp. 1793-1803.
- [36] P. Juszczak, A. S. Kołodziejczyk and Z. Grzonka, “FTIR Spectroscopic Studies on Aggregation Process of the  $\beta$ -Amyloid 11-28 Fragment and Its Variants,” *Journal of Peptide Science*, Vol. 15, No. 1, 2009, pp. 23-29. [doi:10.1002/psc.1085](https://doi.org/10.1002/psc.1085)